From Interference Mitigation to Toleration: Pathway to Practical Spatial Reuse in LPWANs

Ruonan Li[1], Ziyue Zhang[1], Xianjin Xia[1], Ningning Hou[2]
Wenchang Chai[1], Shiming Yu[1], Yuanqing Zheng[1], Tao Gu[2]
[1] The Hong Kong Polytechnic University, Hong Kong, China
[2] Macquarie University, Sydney, Australia
{ruo-nan.li,ziyue.zhang}@connect.polyu.hk,xianjin.xia@polyu.edu.hk,ningning.hou@mq.edu.au,
{wenchang.chai,shiming.yu}@connect.polyu.hk,csyqzheng@comp.polyu.edu.hk,tao.gu@mq.edu.au

ABSTRACT

This paper addresses the interference challenges, aiming to improve spatial reuse and optimize spectrum efficiency in LPWANs. We reveal that existing strategies such as interference cancellation and MIMO are ill-suited to the low-cost low-rate characteristics of LPWANs. Our work introduces a novel framework, *HydraNet*, which leverages the capture effect of LPWAN radios to enable robust concurrent transmissions. *HydraNet* exempts from strict clock synchronization or accurate channel estimation as required by conventional spatial reuse strategies for interference nulling. We conduct in-depth studies with LoRa radios to uncover their underlying packet reception mechanisms and for the first time characterize their unique capture effect. Based on the new findings, we devise novel strategies to jointly control the timing and power of concurrent LPWAN transmissions. These strategies ensure sufficient power differences between packets and interference at their intended receivers. We prototype *HydraNet* and integrate with operational LoRaWANs and comprehensively evaluate its performance. Results show that *HydraNet* achieves higher spectrum utilization with up to 3.6 × throughput improvements over the state-of-the-art.

CCS CONCEPTS

• **Networks** → **Network protocol design**; • **Computer systems organization** → *Embedded systems.*

KEYWORDS

LPWAN, spatial reuse, interference mitigation, concurrent communication

Permission to make digital or hard copies of part or all of this work for personal or classroom use is granted without fee provided that copies are not made or distributed for profit or commercial advantage and that copies bear this notice and the full citation on the first page. Copyrights for third-party components of this work must be honored. For all other uses, contact the owner/author(s).

ACM MobiCom'25, November 3–7, 2025, Hong Kong, China
© 2025 Copyright held by the owner/author(s).
ACM ISBN 979-8-4007-1129-9/25/11
https://doi.org/10.1145/3680207.3723483

ACM Reference Format:
Ruonan Li[1], Ziyue Zhang[1], Xianjin Xia[1], Ningning Hou[2], Wenchang Chai[1], Shiming Yu[1], Yuanqing Zheng[1], Tao Gu[2] . 2025. From Interference Mitigation to Toleration: Pathway to Practical Spatial Reuse in LPWANs. In *The 31st Annual International Conference on Mobile Computing and Networking (ACM MobiCom '25), November 3–7, 2025, Hong Kong, Hong Kong*. ACM, New York, NY, USA, 16 pages. https://doi.org/10.1145/3680207.3723483

1 INTRODUCTION

Low-Power Wide-Area Networks (LPWANs), including LoRa [48, 73, 82], Sigfox [8], and NB-IoT [67], have gained significant traction in recent years [40, 53, 72, 77, 78]. LPWANs complement existing technologies like Wi-Fi and 5G by offering cost-efficient IoT connectivity over long distances (*e.g.*, tens of km [10]). However, the long communication ranges of LPWANs introduce substantial interference and degrade spectrum efficiency, especially in scenarios with dense deployments of many nodes and gateways [28, 32, 56, 65, 83]. This challenge arises primarily because an LPWAN packet requires a relatively long transmission time, during which a single packet transmission can affect a large area (*e.g.*, tens of km^2), monopolizing a frequency band and preventing other nodes in the vicinity from using the same band. Although current LPWANs allow multiple nodes to transmit concurrently using different frequencies and orthogonal parameters, these techniques demand additional resources (*i.e.*, multiple frequencies and orthogonal codes). Our research aims to enhance the spectrum efficiency of LPWANs by exploring the spatial reuse of available spectrum resources, enabling more users to transmit simultaneously on the same frequency.

A core problem in spatial reuse is managing interference among simultaneous transmissions. Existing solutions can be classified into three categories [2, 84]: interference avoidance (*e.g.*, LMAC [21]), interference cancellation (*e.g.*, CIC [57]), and multi-antenna techniques (*e.g.*, MU-MIMO). They share a common philosophy, *i.e.*, *interference mitigation*, which aims to reduce interference strength below some thresholds that allow a receiver to treat interference as background noise (see Figure 1). However, interference avoidance strategies typically result in marginal improvements in spectrum efficiency. Interference cancellation, while more effective,

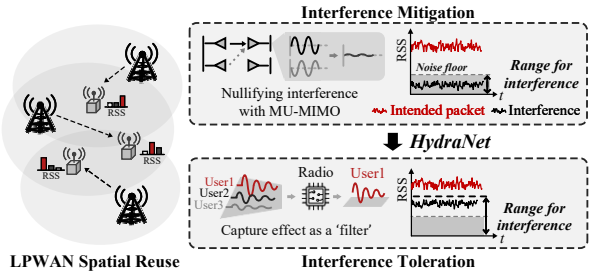

Figure 1: A new framework for LPWAN spatial reuse leveraging radio's capture effect.

requires specialized hardware and complicated signal processing algorithms. This requirement limits spatial reuse in the uplink direction by using customized gateways, while deployed COTS LoRa nodes cannot benefit from concurrent transmissions in the downlink. In contrast, MU-MIMO is capable of operating on the gateway side to facilitate concurrent transmissions for both uplink and downlink in traditional wireless systems. However, our studies in § 2 reveal that MU-MIMO is not well-suited for LPWANs mainly because the slow rate and long air-time of LPWAN packets incur significant delays that can make the channel estimations outdated by the time communication occurs.

This paper presents a new paradigm to facilitate simultaneous LPWAN transmissions on the same frequency, fundamentally evolving the current philosophy of interference management—from mitigating interference to tolerating its presence, as illustrated in Figure 1. We leverage the observation that an LPWAN packet can be successfully received in the presence of interference. This is due to the *capture effect* occurring at the radio circuits, which allows a radio to receive a stronger packet when multiple packets arrive simultaneously [44, 68]. As such, we can maintain a relatively higher Received Signal Strength (RSS) for a desired packet and use the capture effect of a receiver radio as a 'filter' to get rid of interference, even when the interference power is high above the noise floor. Unlike existing spatial reuse solutions that aim to reduce the absolute power of interference below certain thresholds, our approach only needs to suppress interference to be weaker than the desired packet. This significantly relaxes the requirements for interference management and opens up more opportunities for spatial reuse. Importantly, since our approach only manages the power strength of the desired packets and interference, such power features (*i.e.*, RSS) are readily accessible on any COTS devices for both gateways and IoT end-nodes and remain relatively stable over time (see § 3). These make our approach promising for delivering robust spatial reuse in LPWANs, particularly for supporting concurrent downlink transmissions with COTS devices without requiring hardware or software modifications.

To implement this concept into a practical system, two technical challenges must be addressed. First, since our method does not eliminate interference, a radio may perceive multiple packets that contend for radio resources. However, packet reception influenced by the capture effect often exhibits randomness and unpredictability. It is challenging to reliably receive an intended packet amid competing packets. Our comprehensive studies with COTS LoRa radios reveal that the synergy between the PHY-layer capture effect and the higher-layer processing pipeline of a packet receiver jointly determines the reception behavior of a LoRa radio. While the RSS of incoming packets affects the PHY-layer capture effect, the timing of these packets influences the higher-layer receiving pipeline. To mitigate the unpredictability of packet reception associated with the capture effect, it is essential to maintain a higher RSS for the intended packet and control transmission timing among competing packets. This dual approach enables a LoRa radio to effectively capture and receive intended packets amidst interference.

The second challenge involves managing interference among concurrent users. Although our method can tolerate interference with the capture effect, it still requires that the interference power be kept a few dB below the intended packet. Maintaining superior RSS for intended packets against interference at every receiver turns out to be both crucial and challenging. To address this, we jointly leverage the spatial diversities of distributed gateways and transmission power control to manage interference across different subregions. Additionally, we exploit the beamforming capability of multi-antenna gateways to selectively strengthen signal power toward intended users and weaken it in other directions for non-intended users. By jointly optimizing the transmission power of beams and their directions, we can suppress interference at every receiver within a reasonable range, effectively activating the capture effect of receiver radios for correct packet reception.

Finally, we develop a novel communication framework, *HydraNet*, which leverages the PHY capture effect to achieve spatial reuse for LPWANs. A key enabler of *HydraNet* is a spatial reuse protocol that seamlessly integrates with the LoRaWAN stack and utilizes Class B for implementing control plane and data plane operations. *HydraNet* manages concurrent users by grouping them into various spatial reuse groups. To facilitate transmissions for each user group, *HydraNet* initiates a link probing operation to gather essential data of user links (*e.g.*, power fading rates and user directions). This probed data is then fed into an optimization model to compute a transmission plan for users. The plan includes detailed configurations, such as transmit power, beamforming angles, and transmission timing, which are distributed to relevant gateways and user nodes to execute data transmissions within LoRaWAN networks.

We implement a *HydraNet* system using USRP-based gateways and COTS LoRa nodes. Extensive experiments are conducted to evaluate *HydraNet* across diverse link conditions. Results show that *HydraNet* supports a higher number of concurrent users and offers higher reliability than MU-MIMO in both uplink and downlink transmissions. The achieved throughput outperforms that of the state-of-the-art by up to 3.6 ×. *HydraNet* is compatible with single-antenna gateways, with more antennas providing additional spatial reuse opportunities, resulting in 2.4 × throughput improvements as the number of antennas per gateway increases from 1 to 4.

We summarize the contributions of the paper as follows: (1) We systematically investigate the LoRa capture effect and characterize the underlying mechanisms governing the reception behaviors of COTS LoRa radios. This characterization study reveals the joint impact of transmission timing and power control on the unique LoRa capture effect. (2) We propose a novel framework to enable spatial reuse in LPWANs by leveraging the LoRa capture effect. The framework effectively manages interference to ensure sufficient power differences between packets and interference at intended receivers for correct capturing of their packets. (3) We integrate the strategy with the LoRaWAN stack and evaluate its effectiveness through extensive experiments. We believe the design principles of this work could be applied to other LPWAN technologies as well.

2 WHY TRADITIONAL MU-MIMO NOT APPLICABLE TO LPWAN?

Multi-User Multiple Input Multiple Output (MU-MIMO) techniques are commonly used in wireless systems to support multiple users with the same frequency for enhanced spectrum efficiency. MU-MIMO needs to estimate the Channel State Information (CSI) between multiple transmit antennas and receivers to precode the concurrent transmissions of different users. Accurate channel estimation and precoding are essential to ensure only the desired signal can reach the intended receiver, while unwanted signals are nullified through over-the-air transmissions.

To assess the effectiveness of MU-MIMO in LPWANs, we set up a testbed consisting of a two-antenna gateway and multiple Commercial Off-The-Shelf (COTS) LoRa nodes. The two-antenna gateway was constructed using two synchronized USRPs powered by a shared clock, while each LoRa node was equipped with a single antenna. In each experiment, two random nodes were selected to concurrently receive downlink packets from the gateway through a MU-MIMO approach. We employed the methods presented in [50] for real-time channel estimation and precoding (*i.e.*, Zero Forcing encoding [24, 61]). The packet reception ratios (PRRs) of the MU-MIMO communications are presented in Figure 2a. We surprisingly observed that more than 50 % of the nodes failed to receive 80 % of their packets.

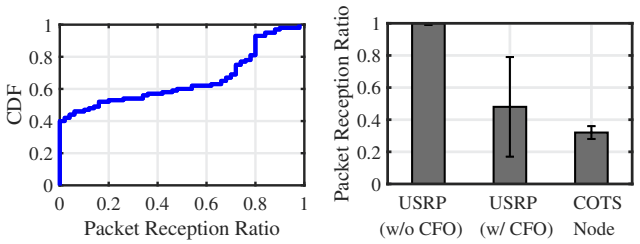

(a) COTS node performance **(b) CFO study**

Figure 2: MU-MIMO performance with LoRa.

Upon reviewing the experimental settings and data, we identified that the low-cost hardware of COTS LoRa nodes, such as the Semtech SX1276 radio [55], introduces Carrier Frequency Offset (CFO) [42] between the sender and the receiver, and different nodes can have different CFOs with the gateway. Although CFO calibration algorithms [74] can rectify received signals to some extent, they suffer unsatisfactory accuracy due to the inherently low quality of signals from low-cost LoRa radios, often leaving random residual CFO errors. The residual CFO errors can compromise CSI measurements, with heterogeneous phase and amplitude variations over different links (refer to Figure 4), and undermine MU-MIMO performance for LoRa nodes.

To access CFO and its impacts on MU-MIMO, we conduct experiments and compare two setups: one with high-end USRPs using local clocks as receivers (with CFO) and another with USRP receivers synchronized to the gateway's clock (without CFO). As shown in Figure 2b, the USRP setup without CFO achieves a perfect 100 % PRR, demonstrating that our methods can accurately measure CSI and facilitate MU-MIMO under ideal conditions. However, in the USRP setup with CFO, where CFO calibration algorithms [74] are used, PRRs significantly drop to 48%, only marginally better than the 32% PRRs of COTS LoRa nodes. This result indicates that CFO calibration cannot totally mitigate the impacts of CFOs. Since LoRa packets have long air-time, even minor CFO errors (*e.g.*, a few Hz) can accumulate over time, resulting in substantial degradation in PRRs.

In addition to CFOs, potential changes in channel conditions (*i.e.*, channel dynamics) can also cause previous CSI measurements to become outdated, leading to incorrect MIMO precoding and degraded performance. Specifically, because multiple LoRa packet exchanges (each lasting hundreds of milliseconds) are required to complete CSI measurements for multiple MIMO links, the time delay between CSI measurement and MIMO communication can span several thousand milliseconds. Meanwhile, a LoRa channel at 915 MHz remains coherent for only a few hundred milliseconds, even when the channel changes at slow speeds (*e.g.*, human walking at 1 m/s). Therefore, acquiring accurate, up-to-date CSI measurements in LPWANs to enable correct MIMO precoding is extremely challenging, if not impossible.

It is important to note that MU-MIMO in traditional wireless systems (*e.g.*, Wi-Fi and LTE) also face challenges related to CFOs and channel dynamics. However, the fast rates of Wi-Fi/LTE transmissions ensure that both CSI measurement and MIMO communication can finish within the coherence time of wireless channels (typically a few hundred milliseconds). In contrast, a single LoRa transmission can last for hundreds of milliseconds, and it takes thousands of milliseconds to complete CSI measurements for multiple LoRa links. Such long intervals necessitate much higher synchronization precision to empower MIMO in LoRa, which can be technically and economically unfeasible for low-cost IoT devices. This challenge motivates us to explore new designs tailored to the unique characteristics of LPWANs to achieve spatial reuse similar to MU-MIMO without demanding strict synchronization.

3 EMBRACING LPWAN INTERFERENCE

Opportunity: Due to the *capture effect* of RF radios, a wireless receiver can sometimes receive one packet intact even when multiple users transmit packets simultaneously, rather than dropping all collided packets [68]. This phenomenon is also observed in LoRa communications with COTS devices, including both gateways and end-nodes across various LoRa radio models such as the SX1272, SX1276, and SX1302, as shown in Figure 3 (refer to § 4.2 for detailed experimental settings). The key observations are summarized below.

(1) COTS LoRa nodes can successfully receive the strongest of the colliding packets. Notably, a RSS difference of 0.8 dB can ensure that a LoRa node reliably receives the stronger packets with ≥90 % PRRs, as shown in Figure 3a.

(2) COTS LoRa nodes can correctly receive an intended packet even when the interference has a strong power strength significantly higher than the noise floor (*e.g.*, >6 dB as shown in Figure 3b). Our in-depth analysis in § 4.2 reveals that due to the unique packet demodulation and receiving pipeline of LoRa radios, the timing of packet collisions and their signal strengths jointly affect the packet reception performance.

These observations encourage us to exploit the packet reception opportunity brought by the LoRa capture effect to support concurrent transmissions from a new perspective:

Instead of suppressing interference to zero, one can just reduce interference strength to a few dB *lower than an intended packet. We leverage a radio's capture effect to "filter out" interfering packets and correctly receive intended packets.*

Paradigm transition: Our work aims to establish a new paradigm for concurrent communications in LPWANs based on the capture effect. This involves a fundamental evolution of interference management philosophy, shifting from the complete elimination of interference to tolerating its presence. Unlike conventional MU-MIMO, our approach does not require precise CSI measurements or MIMO precoding to mitigate interference, which demands strict synchronization.

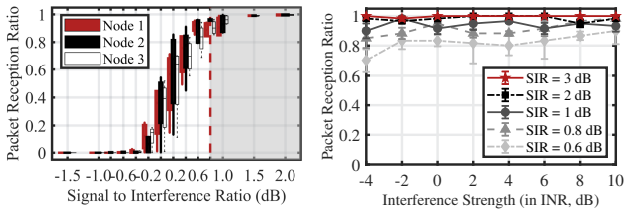

Figure 3: Receiving LoRa packets under different SIR settings (left) and interference strengths (right).

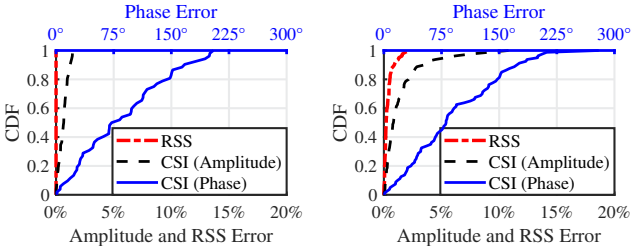

(a) Static links **(b) Dynamic links**

Figure 4: RSS and CSI variations (ground-truth is obtained from USRP devices under ideal settings).

Instead, we focus on managing the RSS difference between interference and intended packets to meet the capture effect SIR threshold of LPWAN radios, ensuring correct packet reception amid interference across different receivers.

We note that the RSS features of packets are inherently resilient to CFOs and remain stable for relatively long periods. Figure 4 experimentally compares the RSS and CSI variations within a LoRa packet duration (*i.e.*, 500∼1000ms). The results show that CSI data, especially the phase measurements, experience significant variations (*e.g.*, up to 200°). Such significant CSI errors can undermine MIMO precoding, resulting in ineffective interference mitigation. In contrast, RSS remains much more stable than CSI measurements in both static and dynamic scenarios. Additionally, we can explore a design space to proactively manage transmission power and select user links with large RSS differences to counteract potential channel dynamics, increase capture effect opportunities, and improve spatial reuse for LPWANs. Importantly, the capture effect is available for almost all LPWAN radios and the RSS readings of packets are also accessible on COTS devices. Our approach is compatible with low-cost IoT devices and holds promise for achieving practical spatial reuse in LPWANs.

4 *HYDRANET* DESIGN

4.1 Overview

This section introduces *HydraNet* that leverages the PHY capture effect to enable spatial reuse of spectrum resources for LPWANs. *HydraNet* operates as follows: When N users need to communicate simultaneously, we first probe the power fading characteristics of the links between user nodes and

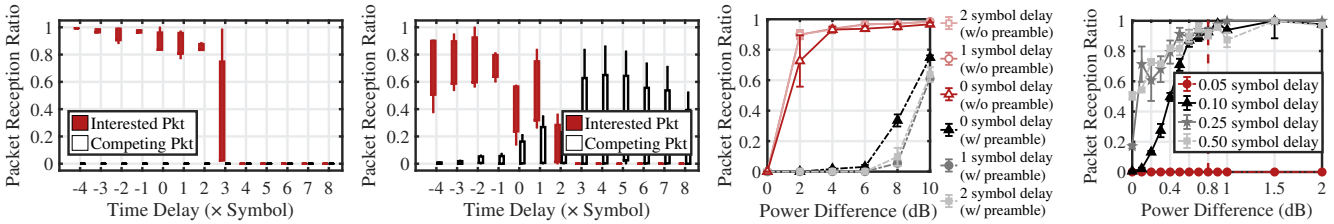

(a) 2 dB **power difference** **(b)** 0.4 dB **power difference** **(c) Symbols aligned** **(d) Symbols not aligned**

Figure 5: Reception with LoRa capture effect when an interested packet is stronger than a competing packet by (a) 2 dB **and (b)** 0.4 dB**, where the symbol timing of the two packets are randomly aligned; PRRs of the interested packet when (c) two packets are aligned and (d) not aligned.**

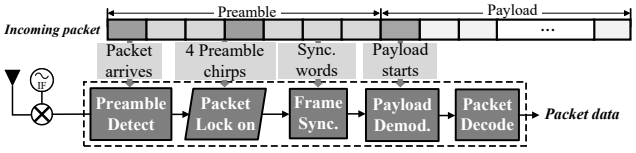

Figure 6: Processing logic of a LoRa packet receiver.

LPWAN gateways and assign various gateways to serve the N users. To ensure successful packet delivery, we carefully control the transmission timing and power for each user so that the signal strength of each packet at its intended receiver is higher than that of any non-intended packets (*i.e.*, interference), without necessarily suppressing the interference power to zero. On the receiver side, an LPWAN radio leverages the PHY capture effect to successfully receive the intended packet with higher signal strength while rejecting non-intended packets with lower strength.

The practical implementation of the system presents two key challenges. First, the success of *HydraNet* depends heavily on the reliable reception of packets via the capture effect. Therefore, a deep understanding of the LoRa capture effect, which is still under-explored in the literature, is essential and will be addressed in § 4.2. Second, as N users communicate simultaneously, each receiver node may receive all N packets at differing signal strengths. While increasing the transmission power of a packet can help its intended receiver capture and decode it, this also increases interference at non-intended receivers, potentially hindering their ability to receive their own packets. Managing interference across concurrent links to ensure all users successfully receive their intended packets is a significant challenge, which we address with novel techniques in the following subsections (§ 4.3).

4.2 Reliable Reception with Capture Effect

The capture effect is an inherent phenomenon in Frequency Modulated (FM) radios, occurring at the signal limiter circuits and during the demodulation stage of a receiver radio [37]. When multiple signals of unequal power strengths fall within the passband of a radio, weaker signals experience higher attenuation than stronger ones as they pass through the radio circuits (*e.g.*, mixer, filter) and often do not appear in the radio's output. However, the PHY layer capture effect often exhibits high variability [36]. The ability of a radio to receive packets through the capture effect varies across technologies, depending on factors such as PHY (de)modulation schemes and radio circuits. This section investigates the capture effect in LoRa radios and provides insights into how to reliably receive packets using this effect.

To study the capture effect, we set up an experiment using three COTS LoRa nodes: two senders and one receiver. One sender transmits a stronger packet (*i.e.*, the packet of interest), while the other sends a weaker competing packet concurrently to the same receiver. By varying the time delay between the transmissions of the two packets, we observe how they are received by the receiver. As shown in Figure 5a and 5b, a LoRa radio exhibits distinct reception behaviors under different delay and power settings. This variability arises because different delays cause different parts of the two packets to collide, and the receiver may capture and receive signals from different packets at different time windows. Additionally, a LoRa radio executes a pipeline to receive a packet, as shown in Figure 6. The receiver pipeline detects a preamble signal to identify a packet. Upon detecting a preamble in several consecutive windows (*e.g.*, four windows for SX1276 [29]), the pipeline locks on that packet to demodulate and decode its payload. The capture effect of radio hardware and the processing logic of the receiver pipeline jointly decide the reception behavior of a LoRa node, as shown in Figure 7 and explained below in three cases.

Case A: When the interested packet arrives before the competing packet, the competing packet collides with the later part of the interested packet. The radio will capture and receive the stronger symbols from the interested packet in every time window, resulting in successful reception of the interested packet (Figure 5a when delay < 0).

Case B: When the interested packet arrives after the competing packet but before the fourth symbol of the competing packet, the radio has not yet locked on the competing packet. The capture effect makes the radio lock on the late stronger interested packet, resulting in high reception ratios for the interested packet (Figure 5a when delay $0 \sim 2$).

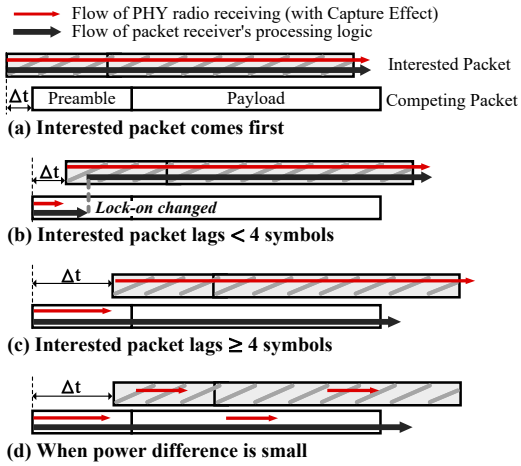

Figure 7: Radio receive behaviors with capture effect.

Case C: When the interested packet arrives after the fourth symbol of the competing packet, the radio locks on the competing packet in the first part but captures/receives stronger symbols from the interested packet in the second part, leading to failures of both packets (Figure 5a when delay > 3).

Comparing Figure 5a and Figure 5b, we observe that fewer interested packets are received as the power difference between the two packets is small (*e.g.*, 0.4 dB). In such cases, the capture effect becomes unpredictable, and the receiver radio may rapidly switch between packets (see Figure 7d), increasing the uncertainty of packet reception.

To identify the power and timing conditions for reliable packet reception with the LoRa capture effect, we vary the time delay between the competing packet and the interested packet from 0 to 3 symbols, precisely control their symbol timing to be well-aligned or misaligned, and adjust their power difference in 0.1 dB increments. Interestingly, the results differ significantly depending on whether the symbol edges of the two packets are aligned or misaligned, as shown in Figure 5c and Figure 5d. When the symbol edges are aligned, the receiver node fails to receive the interested packet even when the interested packet is 10 dB stronger than the competing packet. Comparing the results with and without preamble in Figure 5c, where the "w/o preamble" experiments set up the competing packet without a preamble and ensure the receiver node always locks on the preamble of the interested packets, we can identify that the preamble processing of a LoRa receiver requires high SIRs to function correctly in the case of symbol well-alignment. In contrast, when the symbols are misaligned by ≥10 % of a symbol duration, a 0.6 dB power difference results in ≥90 % PRRs of the interested packet.

Why small SIR threshold for LoRa? We note that the capture effect alone requires a large SIR (*e.g.*, >10 dB) to completely suppress interference signals in the output of a LoRa radio. As SIR decreases (*i.e.*, interference power increases),

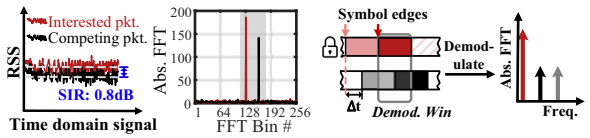

(a) LoRa demodulation **(b) Timing misalignment**

Figure 8: (a) LoRa demodulation and (b) demodulation of misaligned symbols.

the interference signals cannot be suppressed by the capture effect and will flow into the follow-up receiver pipeline of a LoRa radio along with the interested signals. In this case, the LoRa radio can still correctly receive the interested packet amidst interference with SIRs as low as 0.8 dB. This strong interference resistance capability can be explained from the perspectives of LoRa demodulation and the packet receiving pipeline, as detailed below.

LoRa demodulation involves a Dechirp-and-FFT procedure [31, 75] that amplifies a small SIR into a relatively large energy difference for the demodulated symbols in FFT views, as shown in Figure 8a. A LoRa demodulator extracts only the highest energy peak as the demodulation result and discards other lower peaks (*e.g.*, the peak from interference). This helps a LoRa radio to correctly demodulate interested packets in the presence of interference without needing to reduce interference below the SIR threshold of the capture effect (*e.g.*, >10 dB). Based on our empirical studies presented in Figure 5d, the minimum SIR threshold required by a LoRa demodulator is around 0.8 dB.

Notably, the small SIR threshold of LoRa necessitates a relatively large symbol timing misalignment between the interested and competing packets (*e.g.*, ≥10 %). Specifically, SIR influences various processing stages of the LoRa receiver pipeline, including signal compensation for CFOs and channel impacts, symbol synchronization, preamble lock-on, and demodulation procedures [6, 76]. In the symbol-aligned case, the energy peaks of two preambles fall within the same frequency bin. From such combined signals, a receiver cannot accurately estimate and calibrate CFOs for the interested packet. This can lead to failures in preamble lock-on or frame synchronization, resulting in erroneous packet reception. Conversely, in the misaligned case, the preambles of two packets are separated in frequencies. A receiver can easily extract the highest frequency peaks that correspond to the interested packet, enabling correct packet lock-on and processing even with low SIRs.

Upon locking on the interested packet, a LoRa demodulator aligns with the symbol edges of the interested packet while spanning across the symbol edges of the interfering packet, as illustrated in Figure 8b. Note that the adjacent symbols in the payload are likely to be different due to the whitening and encoding procedures of a LoRa packet [30, 80]. Large timing misalignment allows the demodulator to accumulate all signal power of a symbol into a high-energy peak

for the intended packet while dispersing the signal power from the interfering packet into different symbol frequencies, each becoming even lower. This further helps payload demodulation for the interested packet with small SIRs.

Reliable reception conditions. Based on the above experimental results, we empirically conclude the conditions required to empower a LoRa node to reliably receive a packet with the LoRa capture effect as follows:

R1: The transmission of the interested packet must not lag behind any competing packet by more than three symbols.

R2: The symbol timing of the interested packet must be misaligned with that of any competing packet by ≥10 % of a symbol duration.

R3: The RSS of the interested packet must be at least 0.8 dB higher than the RSS of any competing packet.

4.3 Interference Tolerable Spatial Reuse

This section presents a novel framework for enabling spatial reuse in LPWANs by tolerating, rather than eliminating, network interference. The key enabler of this method is a scheduler that coordinates user transmissions to activate the capture effect of receiver radios at the right moment, allowing them to correctly capture and receive intended packets while rejecting non-intended packets (*i.e.*, interference). To ensure reliable packet reception via the LoRa capture effect, the timing and power strength of user transmissions must be carefully controlled, according to the conditions summarized at the end of § 4.2. While controlling transmission timing is technically feasible for LPWANs (addressed in § 4.4), this subsection focuses on managing interference power across user transmissions. We first introduce the basic problem and solutions for typical LPWAN scenarios with distributed single-antenna gateways, followed by an exploration of spatial reuse opportunities with multi-antenna gateways. Finally, we extend the framework to support both uplink and downlink transmissions.

4.3.1 Cooperating Distributed Gateways for Spatial Reuse. Figure 9a illustrates a typical LPWAN network with multiple gateways, each equipped with a single antenna, operating in a shared spectrum. Our objective is to enable these distributed gateways to collaboratively transmit data to various users over the same frequency. To achieve this, the spatial diversities of distributed gateways and transmission power control are jointly utilized to manage interference among user transmissions. It involves two key decisions: (1) which gateway is assigned to serve each user, and (2) the configurations of transmission power (*i.e.*, Tx power) for each gateway.

Unlike conventional spatial reuse schemes [84] that use power control to ensure the signal strength of a packet at non-intended receivers (*i.e.*, interference) remains below the minimum SINR allowed by a radio, *HydraNet* permits interference above the SINR threshold. It only requires the RSS of the intended packets to be relatively higher than that of the

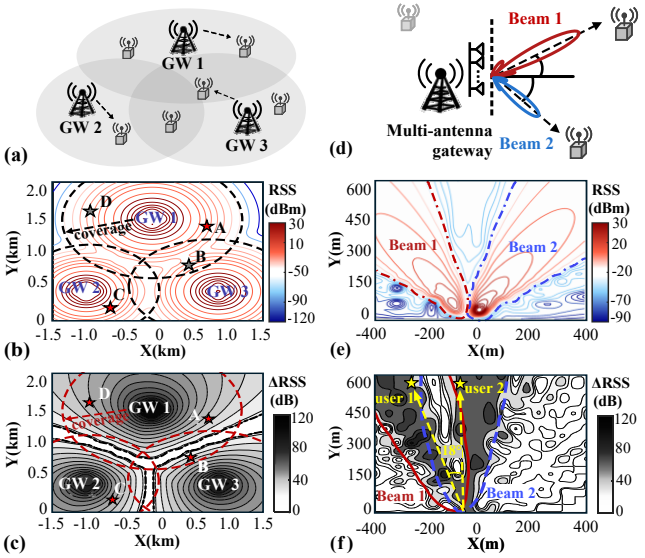

Figure 9: Managing interference for spatial reuse: traditional power control (b) vs. power control in *HydraNet* (c); traditional beamforming (e) vs. power beams in *HydraNet* (f). (b,e) plot the raw RSS of gateways/beams; (c,f) plot the regions, with $\Delta RSS \geq 0.8$ dB, dominating by different gateways/beams.

interference, so that the capture effect of the receiver radio can be activated effectively. This relaxes the requirements for interference management, which can release more spatial reuse opportunities for *HydraNet*. For example, Figure 9b and 9c compare the two methods when using three gateways to serve three users. Traditional power control requires adjusting the coverage of each gateway to mitigate interference at non-intended receivers. It supports two users (*i.e.*, A and C). In contrast, our method supports three users (A, B, and C) with the same Tx power settings for the three gateways.

We formally model the interference management problem in *HydraNet* as an *Interference Tolerable Power Control (ITPC) problem* as follows.

Problem formulation: Assume there are M gateways, represented as $GW = \{g_1, g_2, \cdots, g_M\}$. Denote the receiver nodes of N users as $ND = \{n_1, n_2, \cdots, n_N\}$. The power fading rates for all gateway-to-node links, denoted by $\Gamma_{M\times N}$, are measured beforehand through a link probing process (see details in § 4.4). The ITPC problem computes a *transmission plan* which is formally represented by an association matrix between gateways and users $C_{M\times N}$, where $c_{ij} = 1$ if the i^{th} gateway serves the j^{th} user and 0 otherwise, and a vector $P_{M\times 1}$ recording the Tx power of each gateway. A feasible plan is subject to the following constraints:

- A user is served by at most one gateway: $\forall j,\ \sum_i c_{ij} \leq 1$.
- The Tx power of a gateway cannot exceed the maximum emitting power of the radio (a constant denoted by P_{max}): $\forall i,\ 0 \leq p_i \leq P_{max}$.

- The RSS of a packet at an intended receiver must be higher than a threshold RSS_0: $\forall i, j,\ c_{ij} \cdot RSS_{ij} \geq RSS_0$, where RSS_{ij} is the RSS of a packet from gateway g_i to node n_j calculated by $RSS_{ij} = p_i - \gamma_{ij}$, where γ_{ij} is the power fading rate (in dB) of the link from g_i to n_j.
- A node receives its intended packet with higher RSS than other packets: $\forall i, j, k, (k \neq i),\ c_{ij} \cdot (RSS_{ij} - RSS_{kj}) \geq c_{ij} \cdot \eta_0$, where η_0 is the RSS guard (0.8 dB) required for reliable packet reception with the LoRa capture effect.

Our optimization objective is to maximize the number of concurrent users which can be formulated as below.

$$Maximize \sum_{j=1}^{M} \sum_{i=1}^{N} c_{ij}. \quad (1)$$

4.3.2 Enhancing Spatial Reuse with Multi-antenna. Although the interference-tolerable power control (ITPC) method allows distributed gateways to communicate concurrently in a common space, the spatial reuse opportunity remains limited. It cannot support the concurrent transmissions of two users if they are both located in the same region with superior RSS dominating by the same gateway, such as A and D in Figure 9c. We aim to overcome this barrier by leveraging the multi-antennas available on the latest LPWAN gateways (*e.g.*, Wisgate RAK7289CV2 [52]).

Intuitively, we can treat each multi-antenna element as an independent transmitter and use a greater number of transmitters to support more concurrent users. However, this method cannot transform the increased number of transmitters into higher spatial reuse because all antenna elements are mounted on a gateway within a small space (*e.g.*, tens of cm). The close proximity of multi-antenna elements won't cause substantial RSS variations compared to a single-antenna and thus fails to bring new spatial reuse opportunities. Our empirical results show that, two antennas need to be separated by tens of meters to produce sufficient RSS variations to enable spatial reuse.

We present a novel technique that leverages the beamforming capability of multi-antenna to generate multiple beams of power radiation, termed *power beams*, as illustrated in Figure 9d . Each power beam can be independently used to send packets to different users. Our power beam method differs from traditional beamforming in both the design principle and the resulting capacity achieved. Specifically, traditional beamforming methods produce relatively wide beams with the sub-GHz LPWAN frequency due to the long wavelength. As illustrated in Figure 9e , beamforming with four antennas operating at 915 MHz produces a beam spanning 28∼58°. It requires large antenna arrays and sophisticated software to narrow the beams and avoid potential inter-beam interference when two users are located closely. In contrast, our method is designed to tolerate inter-beam interference, allowing power beams to overlap and support concurrent users even when they are closely located. As shown in Figure 9f , by using the same four antennas, our method can use overlapping power beams to serve two users with a minimum angle difference of 18°. In comparison, a traditional beamforming method requires 8 antennas to achieve the same angular resolution. Thanks to the interference toleration design principle, our power beam method can use fewer antennas with simpler algorithms to support even more users, making it more suitable for low-cost LPWAN devices.

HydraNet assigns the multiple power beams of every multi-antenna gateway to serve different users by steering each beam toward a specific user. This offers us the flexibility to deliver adequate signal power to an intended user node at any angle while minimizing interference to non-intended users, who are typically located in different directions. *HydraNet* properly allocates the Tx power of multi-antenna across the various power beams to ensure good reliability for all supported users. Compared to the single-antenna ITPC method, our power beam approach introduces two additional dimensions, the number of beams and beam directions, beyond gateway locations and power control in ITPC. These new dimensions enable finely modifying RSS in space across various directions. This enhancement enables more precise and finer interference management among concurrent users, potentially creating more opportunities for spatial reuse.

HydraNet determines the optimal power beam configurations for each multi-antenna gateway by solving an extended version of the ITPC problem. The extended ITPC problem replaces all gateways with power beams. A multi-antenna gateway is represented by K power beams, while a single-antenna gateway is treated as an omnidirectional power beam. The problem involves deciding which beam to use for each user (*i.e.*, beam direction) and determining the Tx power for the beams. The angles of user nodes relative to each gateway are measured beforehand via link probing (see § 4.4). The RSS estimation of a packet with power beams is updated as $RSS = P_{tx} \cdot AG_{tx}(\theta, \varphi) - \gamma_{link}$, where $AG_{tx}(\theta, \varphi)$ [13] models the power gain (in dBi) toward angle φ when the power beam is steered along angle θ, given that the receiver is in angle φ relative to the gateway.

4.3.3 Bi-directional Spatial Reuse. Our framework can be seamlessly extended to support spatial reuse in the uplink direction. Unlike standard LoRaWAN, where an uplink packet is received and relayed by all gateways in the area, our framework enables different gateways to relay uplink packets for different nodes. This is particularly helpful when multiple gateways from different operators are deployed in a common area, as it enables each gateway to exclusively serve nodes owned by its respective operator.

To achieve spatial reuse among uplink users, *HydraNet* employs the same method as in downlink to acquire link data and solve the ITPC problem to compute an optimal transmission plan for uplink. While executing an uplink transmission plan, we need to control the transmission power and timing

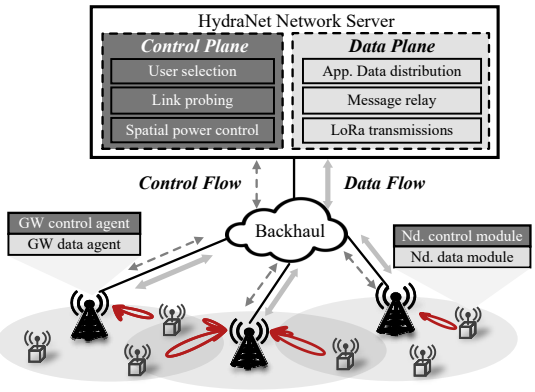

Figure 10: *HydraNet* system overview.

at the node side. A practical challenge is how to control the timing of concurrent uplink transmissions among nodes that are dispersed across different locations. We solve this problem by adding the relevant concurrent nodes into a group and sending a control packet to coarsely synchronize the uplink transmissions among all nodes in the group. Since the transmission timing of concurrent packets in *HydraNet* only needs to be controlled at the symbol level within tens of milliseconds (refer to § 4.2), the synchronization precision of existing LPWAN devices is sufficient to meet our requirements. Lastly, when multi-antennas are available on some gateways, we can also create multiple power beams at the gateway side to support more concurrent users in the uplink. Each power beam would be used to receive uplink packets from a specific node in a particular direction.

4.4 Putting All Together

Figure 10 presents the architecture of *HydraNet* that consists of entities on the cloud server, gateways, and end nodes of a LoRaWAN system. The main functional components run on a centralized network server and are logically divided into a *control plane* and a *data plane*. The control plane manages users participating in concurrent transmissions and performs operations such as link probing and power control to facilitate transmissions. The data plane takes instructions from the control plane and configures gateways and end nodes to transmit data for concurrent users. There are corresponding control plane and data plane modules in the gateway and node sides. The interactions among the network server, gateways, and end nodes are regulated by a protocol.

Spatial reuse protocol. *HydraNet*'s spatial reuse protocol operates in three phases, *i.e.*, user group creation, link probing, and data transmission, as shown in Figure 11. Each phase involves a series of message exchanges (termed a *transaction*) occurring within both the backhaul network and the end LoRa networks.

Group creation: HydraNet organizes user transmissions into *Spatial Reuse Groups (SRG)*. Before transmitting data,

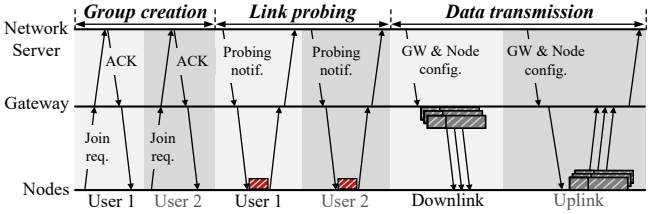

Figure 11: Spatial reuse protocol.

a user node must join an SRG by sending a join request to the network server. The *HydraNet* server responds with an ACK and configures the user node to open specific transmission slots. This setup enables the user node to receive regular downlink messages from the network server, facilitating control plane and data plane operations during the subsequent link probing and data transmission phases.

Link probing: HydraNet conducts link probing to determine the directions of all user nodes relative to each gateway and to measure the power fading rates of the links. A user node is required to send an empty LoRa packet (*i.e.*, the payload is null, containing only a preamble) with a fixed transmit power (*e.g.*, 20 dBm). All gateways passively receive the probing packet. The fading rate of a link can be calculated directly from the received signal strength (RSS) of the packet. Though the link fading rate is measured from an uplink packet, it can be applied to both directions due to the reciprocity of wireless channels [45]. When a gateway is equipped with multiple antennas, it employs the MUSIC algorithm [54] to estimate the Angle-of-Arrival (AoA) of incoming signals, from which user direction can be determined.

Data transmission: A data transmission transaction consists of two sub-stages: data preparation and transmission. The first stage occurs at the network server, which uses the probed link data to compute a transmission plan (*i.e.*, solving the ITPC problem) and sends the detailed transmission settings to the relevant gateways. The second stage involves configuring the relevant gateways (*i.e.*, Tx power, beam directions, and transmission time) to concurrently send data packets in the LoRa network. For uplink data transmissions, the network server sends a message to the relevant end nodes, configuring and synchronizing multiple nodes to send uplink packets concurrently, as illustrated in Figure 11.

Given that link fading rates and node locations do not change frequently in many networks, a single link probing can often be followed by multiple data transmissions to amortize the overheads. *HydraNet* allows link probing to be performed adaptively to balance system efficiency and cost.

Integration with the LoRaWAN protocol. *HydraNet* requires regular downlink transmissions from the network server to end nodes. While LoRaWAN Class A only allows an end node to receive downlink after initiating an uplink transmission, the Class B features of LoRaWAN would be more suitable to support *HydraNet*: A Class-B enabled end

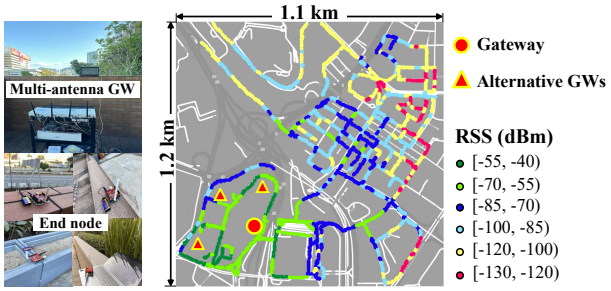

Figure 12: Devices and deployment map of the testbed.

node periodically wakes up to listen to Beacons of gateways, which provide a timing reference to synchronize end-nodes to gateways. LoRaWAN Class B also allows an end node to open up independent downlink windows, termed *ping slots*, to receive network-server-initiated packets at a planned time.

5 EVALUATON

5.1 Methodology

Implementation & Devices. We implement a prototype system of *HydraNet* using a workstation, customized USRP-based multi-antenna gateways, and COTS LoRa nodes. The workstation runs the *HydraNet* server that connects to all gateways via Ethernet. Our customized multi-antenna gateway is built using multiple USRPs (N210) connected to a common external clock (CDA-2990). The gateways run an open-source LoRa protocol, `gr-lora` [16], to communicate with COTS LoRa nodes. The Network Time Protocol (NTP) is used for time synchronization among distributed gateways. *HydraNet*'s spatial reuse protocol operates on both the workstation server and the distributed gateways. The gateways receive instructions from the *HydraNet* server and configure their power beams in real time to communicate with LoRa nodes across various locations. The LoRa nodes consist of Dragino LoRa shields embedded with Semtech SX1276 radio. These LoRa shields are connected to Arduino Uno boards, and the radio chips are configured to send and receive LoRa packets with specific parameters.

Experiment setup. We build a testbed consisting of four gateways and 80 LoRa nodes and conduct extensive experiments over six weeks to evaluate *HydraNet*. The testbed is deployed across a 1.1 km×1.2 km urban area, covering tens of street blocks as shown in Figure 12. The gateways are mounted on the roof of a six-storey building. We collect data traces from over 2,000 links across different locations within the testbed area. The collected data covers a variety of channel conditions (*e.g.*, low and high SNRs, indoor and outdoor, static and dynamic links).

Comparison benchmarks. *HydraNet*'s performance is compared against the following state-of-the-art (SOTA) strategies: (1) LoRaWAN with LMAC [21], the SOTA MAC protocol used to avoid collision in LoRaWAN; (2) MaLoRaGW [50], the latest work applying MIMO techniques in LoRaWAN; (3) CIC

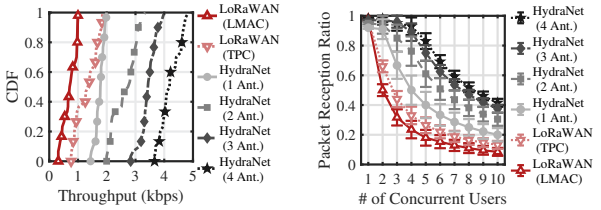

(a) Aggregated throughput **(b) Average PRRs**

Figure 13: Spatial reuse performance of two gateways when 1~4 antennas are equipped per gateway.

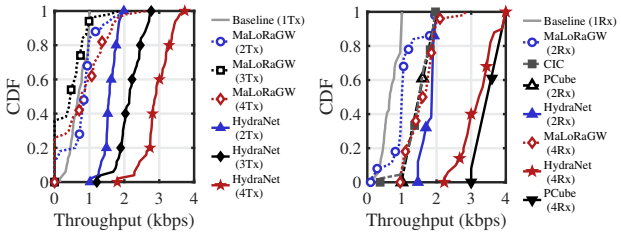

(a) Downlink **(b) Uplink**

Figure 14: Comparing *HydraNet* to SOTA strategies using the same number of transmitters and receivers.

[57], the SOTA on LoRa concurrent interference cancellation; (4) PCube [74], the SOTA on using multi-antenna techniques to resolve LoRa collisions for parallel packet reception.

5.2 On-Site Field Evaluation

Spatial reuse performance. To practically evaluate *HydraNet* 's spatial reuse capability in the testbed area, we set up two distributed gateways, each equipped with 1 to 4 antennas, and configure them to send concurrent packets with a Spreading Factor (SF) 8 and a bandwidth of 125 kHz to varying numbers of users. For each setting of concurrent users, we repeat the experiment 50 times with randomly selected user locations. Two baseline schemes are employed: LoRaWAN (LMAC), which permits only one user to transmit at a time, and LoRaWAN (TPC), which applies an optimal Tx Power Control to the two gateways to achieve spatial reuse. We measure the packet reception ratio of each node and the aggregated throughput of the entire network, as shown in Figure 13. As expected, LoRaWAN (TPC) produces higher throughput than LoRaWAN (LMAC) because it enables spatial reuse between the two gateways via power control. However, the PRRs of LoRaWAN (TPC) for two users remain below 70 %. In contrast, *HydraNet* supports two concurrent users with PRRs greater than 90 %, even when a single antenna is used by the gateways, as shown in Figure 13b. *HydraNet* achieves higher aggregated throughput as more antennas are used. When each gateway has two or more antennas, *HydraNet* creates power beams from the multi-antennas to support more users. The two gateways

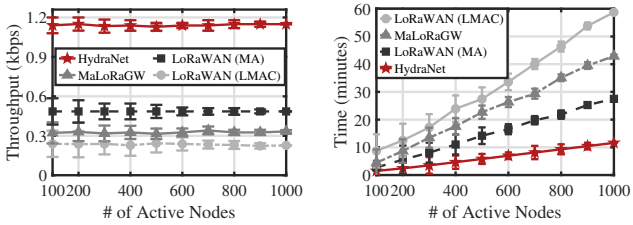

(a) Effective throughput **(b) Completion time**

Figure 15: Scalability performance of applying various strategies to distribute control messages to all nodes.

# of GWs	Antenna per GW	Ctrl. pkts.	Data pkts.	Over-head
4	1	20	2105	0.47 %
2	2	20	2123	0.46 %
1	4	20	2295	0.43 %

Table 1: Link probing overhead of *HydraNet*.

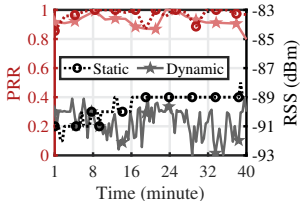

Figure 16: PRR and RSS variations of two links.

can concurrently transfer data for up to five users when each gateway uses four antennas. The achieved throughput is 2.4 × higher than that of the single-antenna settings.

Comparison to state-of-the-art. Next, we compare *HydraNet* with SOTA strategies. Since CIC and PCube are not applicable to downlink transmissions, we only use them for uplink comparisons. In the downlink experiments, we set up 2~4 USRPs connected to the same external clock, serving as synchronized gateway antennas. MaLoRaGW uses these antennas to transfer data to multiple users with MIMO, while *HydraNet* employs our spatial reuse method. The LoRa packet parameters are set to SF8 and Bandwidth 125 kHz. We compare *HydraNet* and MaLoRaGW using the same number of transmitter antennas. As standard LoRaWAN allows only one transmitter to communicate in the testbed area, the throughput of a single transmitter is plotted as a baseline reference. As shown in Figure 14a, MaLoRaGW does not produce significantly higher throughput compared to the single transmitter baseline. This is primarily due to the high inaccuracy of CSI measurements in LoRa links, which results in failed MIMO functionality. In contrast, *HydraNet* doubles the baseline throughput when two transmitters are used, and more transmitters produce even higher throughput. *HydraNet* achieves 3.6 × higher downlink throughput than MaLoRaGW when four transmitters are used.

The same gateway settings, with 2~4 synchronized USRPs as receiver antennas, are used for uplink experiments. We randomly select LoRa nodes from various locations to concurrently send packets. The USRPs receive the PHY signals of the uplink packets and employ different strategies to process these signals for packet decoding. Figure 14b reports the aggregated network throughput of all strategies. We observe that *HydraNet* outperforms CIC by 30.2 % and 133.8 % when using two and four receiver antennas, respectively. Overall, *HydraNet* achieves uplink throughput comparable to PCube when using the same receivers.

Scalability. This experiment evaluates the scalability of *HydraNet* through emulations. We gathered over 20,000 packet traces from the area depicted in Figure 12 and replayed the traffic in our testbed to evaluate *HydraNet*'s performance in supporting real-world, large-scale LoRaWAN communications. We consider a street light control application where each street lamp needs to receive a message (10 Bytes) from a control server to turn on/off the light every evening and morning. We employ two gateways, each equipped with four antennas, to send control instructions to all nodes using various strategies. The end nodes are randomly selected from different locations within the area shown in Figure 12. In our region, LoRaWAN allocates only one frequency channel for downlink communication. The bandwidth of LoRa packets is 125 kHz, and the SF parameter is configured based on the link condition (*e.g.*, RSS) between a node and the gateway. For *HydraNet* and MaLoRaGW, we divide the nodes into various concurrent transmission groups; the nodes within each group use the same SF. We set up two baselines: LoRaWAN (LMAC), which sends downlink packets sequentially to each node one by one, and a multi-antenna enhanced version, LoRaWAN (MA), that uses each antenna to send packets to different users with orthogonal SFs. LoRaWAN (MA) can serve six users at a time, *i.e.*, using SF7~SF12.

Figure 15 compares the throughput of various strategies and the time taken to complete transmitting control instructions for all nodes under different network sizes. As expected, *HydraNet* achieves the highest throughput, approximately 5 times that of LoRaWAN (LMAC). MaLoRaGW offers less than a 50 % throughput improvement over LoRaWAN (LMAC), mainly due to the high failure rate of MIMO with LoRa packets. Since LoRaWAN (MA) only allows concurrent transmissions among nodes using different SFs, the potential for concurrency remains limited in our scenario, resulting in lower throughput than *HydraNet*. *HydraNet* effectively utilizes all antennas to send control instructions to multiple nodes concurrently. It significantly reduces the time required to control 1,000 street lamps from 60 minutes with LoRaWAN (LMAC) to just 10 minutes.

Link probing overhead. This experiment examines the overhead of link probing in *HydraNet*. We choose 10 nodes from the green RSS region of the testbed area (see Figure 12), where all nodes can connect to gateways with SF8. Each node uploads 20 KB data to mimic data reports in smart metering applications [20]. Various gateways are used to enable concurrent transmissions with *HydraNet*. The experiment lasts for nearly one hour. Link probing occurs at the beginning of node transmissions and during transmissions upon detecting high packet losses. We record the number of control

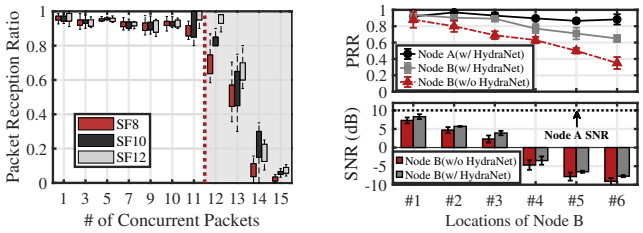

(a) PRRs vs. # of users (b) 2 nodes w/ varying SNRs

Figure 17: Capability study (a); and near-far effect (b).

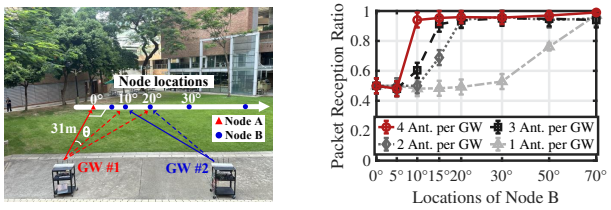

Figure 18: Impact of node proximity: Settings of node locations (left) and *HydraNet* performance (right).

packets and data packets sent by all nodes as presented in Table 1. The overhead is computed as the time ratio of control packet transmissions to all transmitted packets. We see that the link probing overhead remains lower than 0.5 % across all settings. In all our experiments, *HydraNet* initiates only one round of link probing at the start, and the probe data (*i.e.*, node directions and link fading rates) remain effective throughout the entire experiment. Figure 16 presents a snapshot of PRR and RSS changes for two nodes (one node with a static link and the other with a dynamic link) throughout the experiment. Both nodes maintain PRRs of ≥90 % for most of the time, eliminating the need for additional link probing operations. For the node with a dynamic link, although the RSS varies largely (*e.g.*, −93 dBm to −89 dBm), *HydraNet* effectively adapts to the link condition by using a large Tx power and proper beam settings to deliver high PRRs.

5.3 Micro Benchmarks

Capability study. Recall that *HydraNet* leverages the capture effect of LoRa radio to receive packets, which requires a timing misalignment of ≥10 % between concurrent packets to ensure reliable reception (refer to § 4.2). This requirement limits the maximum number of concurrent users. To investigate *HydraNet* 's practical capabilities, we design experiments where N nodes send packets concurrently to a receiver node, with the symbol timing (or edges) of the N packets evenly distributed within a symbol duration. This arrangement creates equal timing misalignment (*i.e.*, $\frac{1}{N}$ of a symbol) between any two adjacent packets. We control the Tx power of the senders to ensure that the desired packet is received with a sufficiently higher RSS (*i.e.*, ≥1 dB) than any competing packets. We increase N from 1 to 15 and measure the PRR of the desired packet under various transmission settings. The results, presented in Figure 17a, indicate that *HydraNet* supports a maximum of 11 concurrent users with SF8. While increasing the SF slightly improves PRRs, it does not significantly enhance the overall capability. The system can support up to 12 concurrent users with SF12.

Near-far effect. This experiment evaluates *HydraNet* 's performance when concurrent users experience different link conditions. We employ two LoRa nodes: Node A, positioned at a fixed location with an SNR of 10 dB, and Node B, placed at various locations where Locations #1 to #3 had Line-of-Sight (LoS) links to the gateways, while Locations #4 to #6 were completely blocked with Non-Line-of-Sight (NLoS) link conditions. Both nodes are configured with the default bandwidth of 125 kHz and SF8. Two gateways, each with two antennas, are used to send concurrent packets to the two nodes with *HydraNet*. The link SNRs and PRRs of Node B at various locations when *HydraNet* is not adopted are also plotted in Figure 17b as a baseline reference. We observe that *HydraNet* enables reliable communication for both nodes (PRR>90 %) even with an SNR difference as large as 6.1 dB (*e.g.*, when Node B is at Location #3). As the delta SNR enlarges for Locations #4 to #6 with NLoS links, Node A consistently receives packets reliably, while Node B experiences improved PRRs compared to the baseline without *HydraNet*. This improvement is attributed to *HydraNet* 's effective allocation of transmission power across the power beams to both nodes. As shown in Figure 17b, the link SNRs at Location #6 increase by 1.4 dB with the use of *HydraNet*, resulting in a 30.7 % improvement in PRR. This demonstrates that *HydraNet* can effectively adapt to NLoS links and fundamentally enhance signal qualities over such links.

Node proximity. This experiment examines the performance of *HydraNet* when concurrent users are in close proximity. We employ two gateways, GW #1 and GW#2 separated by 12 m, transmitting concurrently to two nodes (A and B) with SF8. As shown in Figure 18, Node A is positioned directly in front of GW #1 (at an angle of 0°), while Node B is placed at various locations along the white line, ranging from 0° to 70° relative to GW #1. The number of antennas per gateway is varied from 1 to 4. We measure the overall PRRs of the two nodes under different settings as presented in Figure 18. We see that Node B needs to be placed far away (*e.g.*, ≥ 70°) to achieve reliable concurrent communication with Node A when the gateways use a single antenna. In contrast, Node B can be positioned much closer to A when the gateways are equipped with multiple antennas, thanks to the power beams of *HydraNet*. As more antennas are used, the power beams become narrower, allowing for finer separation of users across spatial angles (*e.g.*, 10° with four antennas).

6 DISCUSSION

Link dynamics. Our experimental studies have demonstrated that *HydraNet* can effectively adapt to diverse practical link conditions, including channel dynamics, multi-path

fading, blockage, and NLoS links. As *HydraNet* manages the signal strength (*i.e.*, RSS) of interference and intended packets to facilitate concurrent user transmissions, the RSS remains relatively stable over practical links. In scenarios with rapid channel changes or fluctuating interference patterns that lead to RSS variations, *HydraNet* can transmit concurrent packets with larger RSS margins by using enlarged SIR thresholds to better tolerate the RSS dynamics of links. Additionally, *HydraNet* adopts designs such as transmission power control and optimized power beams to improve RSS scalability over dynamic links, which can enhance the fundamental signal qualities and SNR conditions of these links.

Synchronization issues. *HydraNet* does not require strict synchronization for CFO calibrations or precise channel measurements. Instead, it probes the power fading rates of links, estimated from the RSS of packets, that are immune to CFOs. However, a coarse time synchronization among concurrent users (end nodes for uplink and gateways for downlink) is needed to control their transmission timing according to the reliability conditions provided in § 4.2. Since the LoRa capture effect can be effectively activated with symbol-level (*i.e.*, millisecond-level) time granularity, the existing LoRaWAN synchronization mechanism can provide the required timing precision for gateways and end-nodes to run *HydraNet*.

Extending to other LPWAN technologies. *HydraNet* is built on the capture effect of wireless radios. Since the capture effect is a general phenomenon observed in various wireless technologies, including NB-IoT and Sigfox, the core principles and working mechanisms of *HydraNet* can also be applied to those LPWAN technologies to facilitate spatial reuse and spectrum optimization. However, the exact SIR thresholds and timing requirements need to be adjusted to adapt to different technologies.

7 RELATED WORK

MIMO. A large body of research has focused on enabling Multiple Input Multiple Output (MIMO) to enhance the capacity of radio links, ranging from theoretical analysis [1, 81] to practical implementations [25, 26, 51]. Previous work has focused on lightweight channel estimation[25], user synchronization [5], and user selection [79, 81] to facilitate real-time and multi-user MIMO in Wi-Fi [5, 58, 62], cellular [59], sensor networks [15], and wireless LANs [17]. Recent efforts extend MIMO to wireless software radio [85] and smart surface [19]. In the realm of LPWANs, Iris [22] utilizes the narrow bandwidth of LPWAN to simplify channel estimation through a customized PHY design. Charm [18] applies MIMO to the uplink of LoRaWANs but requires precise time synchronization among distributed gateways. MALoRaGW [49] adopts a joint MAC and PHY design to implement MU-MIMO for LoRaWANs. Unlike previous strategies, our approach leverages the PHY capture effect to enable concurrent transmissions in LPWANs without the need for strict synchronization or precise CSI acquisition.

Spatial reuse. Spatial reuse (SR) techniques have been extensively studied to enhance IEEE 802.11 network efficiency [4, 14]. Previous work leveraged transmission power control (TPC) [33, 60], directional antenna [43], and data rate adaptation [7, 34, 70] to improve spectrum efficiency. The 802.11ax [9, 41, 47, 63] introduces a spatial reuse protocol that adjusts the power threshold of channel sensing (CCA) to enable more users to access the medium concurrently. In contrast, *HydraNet* maintains a relative signal power difference between the intended packet and interference and leverages the capture effect of LoRa radios to filter out interference.

LoRa concurrent transmissions. Another line of research explores various PHY signal features to resolve LoRa collisions for concurrent packet reception [11, 12, 46]. CoLoRa [66] uses the peak power ratio of chirps after demodulation to differentiate chirps from multiple packets. NScale [64] amplifies the time offsets between colliding packets with non-stationary signal scaling in power domain. PCube [74] combines phase and power features to disentangle collisions in the IQ plane. However, these strategies cannot run on COTS LoRa nodes, where the IQ samples of PHY signals cannot be accessed, limiting their applicability for supporting concurrent transmissions in the downlink. In contrast, *HydraNet* supports bi-directional concurrent transmission while remaining fully compatible with COTS devices.

Capture effect. Many studies [23, 35] have investigated the capture effect, particularly for Wi-Fi and ZigBee. Notably, [38] provides a theoretical foundation for understanding this effect through controlled experiments with a limiter and demodulator. In RFID systems, some studies [39, 71] explore leveraging the capture effect for collision detection and recovery [69]. A recent work [3] exploits the capture effect to establish a synchronous transmission kernel, facilitating consensus in ZigBee networks. The capture effect in LoRa has been experimentally studied in [27]. To the best of our knowledge, our work is the first to harness the capture effect to enable concurrent transmissions in LPWANs.

8 CONCLUSION

This paper presents *HydraNet* to enable concurrent communications in LPWANs based on the unique capture effect inherent in LPWAN radios. We first uncover the mechanisms governing the reception behaviors of LoRa radios and provide guidelines to enable reliable packet reception using the LoRa capture effect. We then design novel strategies to jointly control the transmission timing and power among concurrent users so that intended packets can be captured and interference filtered out. Extensive experiments have demonstrated the effectiveness of *HydraNet*. The core principles and strategies underpinning *HydraNet* may also be applicable to other low-cost low-rate LPWAN technologies.

ACKNOWLEDGEMENT

We sincerely thank our shepherd – Dr. Renjie Zhao, and the anonymous reviewers for their constructive comments and invaluable suggestions that helped improve this paper. This paper is supported in part by Hong Kong GRF under Grant No. 15218022, 15231424, 15211924, and 15206123 and in part by the Macquarie University Research Acceleration Scheme. Xianjin Xia and Yuanqing Zheng are the corresponding authors.

REFERENCES

[1] Shuchin Aeron and Venkatesh Saligrama. 2007. Wireless ad hoc networks: Strategies and scaling laws for the fixed SNR regime. *IEEE Transactions on Information Theory* 53, 6 (2007), 2044–2059.

[2] Shivang Aggarwal, Moinak Ghoshal, Piyali Banerjee, Dimitrios Koutsonikolas, and Joerg Widmer. 2021. 802.11 ad in smartphones: Energy efficiency, spatial reuse, and impact on applications. In *IEEE INFOCOM 2021-IEEE Conference on Computer Communications*. IEEE, 1–10.

[3] Beshr Al Nahas, Simon Duquennoy, and Olaf Landsiedel. 2017. Network-wide consensus utilizing the capture effect in low-power wireless networks. In *Proceedings of the 15th ACM conference on embedded network sensor systems*. 1–14.

[4] Basel Alawieh, Yongning Zhang, Chadi Assi, and Hussein Mouftah. 2009. Improving Spatial Reuse in Multihop Wireless Networks - A Survey. *IEEE Communications Surveys & Tutorials* 11, 3 (2009), 71–91. https://doi.org/10.1109/SURV.2009.090306

[5] Horia Vlad Balan, Ryan Rogalin, Antonios Michaloliakos, Konstantinos Psounis, and Giuseppe Caire. 2013. AirSync: Enabling distributed multiuser MIMO with full spatial multiplexing. *IEEE/ACM Transactions on Networking* 21, 6 (2013), 1681–1695.

[6] C. Bernier, F. Dehmas, and N. Deparis. 2020. Low Complexity LoRa Frame Synchronization for Ultra-Low Power Software-Defined Radios. *IEEE Transactions on Communications* 68, 5 (2020), 3140–3152. https://doi.org/10.1109/TCOMM.2020.2974464

[7] Saad Biaz and Shaoen Wu. 2008. Rate adaptation algorithms for IEEE 802.11 networks: A survey and comparison. In *2008 IEEE Symposium on Computers and Communications*. 130–136. https://doi.org/10.1109/ISCC.2008.4625680

[8] Marco Centenaro, Lorenzo Vangelista, Andrea Zanella, and Michele Zorzi. 2016. Long-range communications in unlicensed bands: the rising stars in the IoT and smart city scenarios. *IEEE Wireless Communications* 23, 5 (2016), 60–67. https://doi.org/10.1109/MWC.2016.7721743

[9] Chi-Kin Chau, Ivan W. H. Ho, Zhenhui Situ, Soung Chang Liew, and Jialiang Zhang. 2017. Effective Static and Adaptive Carrier Sensing for Dense Wireless CSMA Networks. *IEEE Transactions on Mobile Computing* 16, 2 (2017), 355–366. https://doi.org/10.1109/TMC.2016.2557780

[10] Lili Chen, Jie Xiong, Xiaojiang Chen, Sunghoon Ivan Lee, Kai Chen, Dianhe Han, Dingyi Fang, Zhanyong Tang, and Zheng Wang. 2019. WideSee: towards wide-area contactless wireless sensing. In *Proceedings of the 17th Conference on Embedded Networked Sensor Systems* (New York, New York) *(SenSys '19)*. Association for Computing Machinery, New York, NY, USA, 258–270. https://doi.org/10.1145/3356250.3360031

[11] Weiwei Chen, Xianjin Xia, Shuai Wang, Tian He, Shuai Wang, Gang Liu, and Caishi Huang. 2024. Enabling Large Scale LoRa Parallel Decoding With High-Dimensional and High-Accuracy Features. *IEEE Transactions on Mobile Computing* (2024), 1–17. https://doi.org/10.1109/TMC.2024.3517343

[12] Weiwei Chen, Runze Zhang, Xianjin Xia, Shuai Wang, Shuai Wang, and Tian He. 2024. Deepdetangle: Deep Learning-Based Fusion of Chirp-Level and Packet-Level Features for Lora Parallel Decoding. In *2024 IEEE 32nd International Conference on Network Protocols (ICNP)*. 1–11. https://doi.org/10.1109/ICNP61940.2024.10858555

[13] Yi Chen and Chong Han. 2021. On Beamforming Gain Models for Performance Evaluation and Analysis of Narrowband and Wideband Wireless Networks. *IEEE Transactions on Communications* 69, 11 (2021), 7864–7878. https://doi.org/10.1109/TCOMM.2021.3108444

[14] LAN/MAN Standards Committee et al. 2018. IEEE P802. 11ax/D4. 0, Draft Standard for Information technology—Telecommunications and information exchange between systems Local and metropolitan area networks—Specific requirements, Part 11: Wireless LAN Medium Access Control (MAC) and Physical Layer (PHY) Specifications, Amendment 1: Enhancements for High Efficiency WLAN. *IEEE Computer Society* 90 (2018).

[15] Aitor Del Coso, Umberto Spagnolini, and Christian Ibars. 2007. Cooperative distributed MIMO channels in wireless sensor networks. *IEEE Journal on Selected Areas in Communications* 25, 2 (2007), 402–414.

[16] John Doe. 2022. gr-LoRa: An Open-Source LoRa Physical Layer Implementation. https://github.com/user/gr-lora Accessed: 6 Aug 2024.

[17] Mischa Dohler, Athanasios Gkelias, and Hamid Aghvami. 2004. A resource allocation strategy for distributed MIMO multi-hop communication systems. *IEEE Communications Letters* 8, 2 (2004), 99–101.

[18] Adwait Dongare, Revathy Narayanan, Akshay Gadre, Anh Luong, Artur Balanuta, Swarun Kumar, Bob Iannucci, and Anthony Rowe. 2018. Charm: exploiting geographical diversity through coherent combining in low-power wide-area networks. In *2018 17th ACM/IEEE International Conference on Information Processing in Sensor Networks (IPSN)*. IEEE, 60–71.

[19] Manideep Dunna, Chi Zhang, Daniel Sievenpiper, and Dinesh Bharadia. 2020. ScatterMIMO: Enabling virtual MIMO with smart surfaces. In *Proceedings of the 26th Annual International Conference on Mobile Computing and Networking*. 1–14.

[20] Commission for Energy Regulation (CER). 2009-2010. CER Smart Metering Project - Electricity Customer Behaviour Trial. https://www.ucd.ie/issda/data/commissionforenergyregulationcer/. Accessed: 2024-08-21.

[21] Amalinda Gamage, Jansen Christian Liando, Chaojie Gu, Rui Tan, and Mo Li. 2020. LMAC: efficient carrier-sense multiple access for LoRa. In *Proceedings of the 26th Annual International Conference on Mobile Computing and Networking* (London, United Kingdom) *(MobiCom '20)*. Association for Computing Machinery, New York, NY, USA, Article 43, 13 pages. https://doi.org/10.1145/3372224.3419200

[22] Chuhan Gao, Mehrdad Hessar, Krishna Chintalapudi, and Bodhi Priyantha. 2019. Blind distributed mu-mimo for iot networking over vhf narrowband spectrum. In *The 25th Annual International Conference on Mobile Computing and Networking*. 1–17.

[23] Cengiz Gezer, Chiara Buratti, and Roberto Verdone. 2010. Capture effect in IEEE 802.15. 4 networks: Modelling and experimentation. In *IEEE 5th International Symposium on Wireless Pervasive Computing 2010*. IEEE, 204–209.

[24] Andrea Goldsmith. 2005. *Wireless Communications*. Cambridge University Press.

[25] Ezzeldin Hamed, Hariharan Rahul, Mohammed A Abdelghany, and Dina Katabi. 2016. Real-time distributed MIMO systems. In *Proceedings of the 2016 ACM SIGCOMM Conference*. 412–425.

[26] Ezzeldin Hamed, Hariharan Rahul, and Bahar Partov. 2018. Chorus: Truly distributed distributed-MIMO. In *Proceedings of the 2018 conference of the ACM special interest group on data communication*. 461–475.

[27] Jetmir Haxhibeqiri, Floris Van den Abeele, Ingrid Moerman, and Jeroen Hoebeke. 2017. LoRa Scalability: A Simulation Model Based on Interference Measurements. *Sensors* 17, 6 (2017). https://doi.org/10.3390/s17061193

[28] Ningning Hou, Xianjin Xia, Yifeng Wang, and Yuanqing Zheng. 2024. One Shot for All: Quick and Accurate Data Aggregation for LPWANs. *IEEE/ACM Transactions on Networking* 32, 3 (2024), 2285–2298. https:

//doi.org/10.1109/TNET.2024.3353792

[29] Ningning Hou, Xianjin Xia, and Yuanqing Zheng. 2021. Jamming of LoRa PHY and Countermeasure. In *IEEE INFOCOM 2021 - IEEE Conference on Computer Communications*. 1–10. https://doi.org/10.1109/INFOCOM42981.2021.9488774

[30] Ningning Hou, Xianjin Xia, and Yuanqing Zheng. 2023. CloakLoRa: A Covert Channel Over LoRa PHY. *IEEE/ACM Transactions on Networking* 31, 3 (2023), 1159–1172. https://doi.org/10.1109/TNET.2022.3209255

[31] Ningning Hou, Xianjin Xia, and Yuanqing Zheng. 2023. Don't Miss Weak Packets: Boosting LoRa Reception with Antenna Diversities. *ACM Trans. Sen. Netw.* 19, 2, Article 41 (Feb. 2023), 25 pages. https://doi.org/10.1145/3563698

[32] Ningning Hou, Xianjin Xia, and Yuanqing Zheng. 2023. Jamming of LoRa PHY and Countermeasure. *ACM Trans. Sen. Netw.* 19, 4, Article 80 (may 2023), 27 pages. https://doi.org/10.1145/3583137

[33] Thomas Huehn and Cigdem Sengul. 2012. Practical Power and Rate Control for WiFi. In *2012 21st International Conference on Computer Communications and Networks (ICCCN)*. 1–7. https://doi.org/10.1109/ICCCN.2012.6289295

[34] Mathieu Lacage, Mohammad Hossein Manshaei, and Thierry Turletti. 2004. IEEE 802.11 rate adaptation: a practical approach. In *Proceedings of the 7th ACM International Symposium on Modeling, Analysis and Simulation of Wireless and Mobile Systems* (Venice, Italy) *(MSWiM '04)*. Association for Computing Machinery, New York, NY, USA, 126–134. https://doi.org/10.1145/1023663.1023687

[35] Jeongkeun Lee, Wonho Kim, Sung-Ju Lee, Daehyung Jo, Jiho Ryu, Taekyoung Kwon, and Yanghee Choi. 2007. An experimental study on the capture effect in 802.11 a networks. In *Proceedings of the second ACM international workshop on Wireless network testbeds, experimental evaluation and characterization*. 19–26.

[36] Jeongkeun Lee, Wonho Kim, Sung-Ju Lee, Daehyung Jo, Jiho Ryu, Taekyoung Kwon, and Yanghee Choi. 2007. An experimental study on the capture effect in 802.11a networks. In *Proceedings of the Second ACM International Workshop on Wireless Network Testbeds, Experimental Evaluation and Characterization* (Montreal, Quebec, Canada) *(WinTECH '07)*. Association for Computing Machinery, New York, NY, USA, 19–26. https://doi.org/10.1145/1287767.1287772

[37] K. Leentvaar and J. Flint. 1976. The Capture Effect in FM Receivers. *IEEE Transactions on Communications* 24, 5 (1976), 531–539. https://doi.org/10.1109/TCOM.1976.1093327

[38] Krijn Leentvaar and Jan Flint. 1976. The capture effect in FM receivers. *IEEE Transactions on Communications* 24, 5 (1976), 531–539.

[39] Bo Li and Junyu Wang. 2011. Efficient anti-collision algorithm utilizing the capture effect for ISO 18000-6C RFID protocol. *IEEE Communications Letters* 15, 3 (2011), 352–354.

[40] Chenning Li, Yidong Ren, Shuai Tong, Shakhrul Iman Siam, Mi Zhang, Jiliang Wang, Yunhao Liu, and Zhichao Cao. 2024. ChirpTransformer: Versatile LoRa Encoding for Low-power Wide-area IoT. In *Proceedings of the 22nd Annual International Conference on Mobile Systems, Applications and Services*. 479–491.

[41] Wei Li, Yong Cui, Xiuzhen Cheng, Mznah A. Al-Rodhaan, and Abdullah Al-Dhelaan. 2011. Achieving Proportional Fairness via AP Power Control in Multi-Rate WLANs. *IEEE Transactions on Wireless Communications* 10, 11 (2011), 3784–3792. https://doi.org/10.1109/TWC.2011.091411.101899

[42] Jansen C. Liando, Amalinda Gamage, Agustinus W. Tengourtius, and Mo Li. 2019. Known and Unknown Facts of LoRa: Experiences from a Large-scale Measurement Study. *ACM Trans. Sen. Netw.* 15, 2, Article 16 (feb 2019), 35 pages. https://doi.org/10.1145/3293534

[43] Xi Liu, Anmol Sheth, Michael Kaminsky, Konstantina Papagiannaki, Srinivasan Seshan, and Peter Steenkiste. 2009. DIRC: increasing indoor wireless capacity using directional antennas. *SIGCOMM Comput. Commun. Rev.* 39, 4 (Aug. 2009), 171–182. https://doi.org/10.1145/1594977.1592589

[44] J. Lu and K. Whitehouse. 2009. Flash Flooding: Exploiting the Capture Effect for Rapid Flooding in Wireless Sensor Networks. In *IEEE INFOCOM 2009*. 2491–2499. https://doi.org/10.1109/INFCOM.2009.5062177

[45] De Mi, Mehrdad Dianati, Lei Zhang, Sami Muhaidat, and Rahim Tafazolli. 2017. Massive MIMO performance with imperfect channel reciprocity and channel estimation error. *IEEE Transactions on Communications* 65, 9 (2017), 3734–3749.

[46] Manan Mishra, Daniel Koch, Muhammad Osama Shahid, Bhuvana Krishnaswamy, Krishna Chintalapudi, and Suman Banerjee. 2023. OpenLoRa: Validating LoRa Implementations through an Extensible and Open-sourced Framework. In *20th USENIX Symposium on Networked Systems Design and Implementation (NSDI 23)*. 1165–1183.

[47] Toshiro Nakahira, Koichi Ishihara, Yusuke Asai, Yasushi Takatori, Riichi Kudo, and Masato Mizoguchi. 2014. Centralized control of carrier sense threshold and channel bandwidth in high-density WLANs. In *2014 Asia-Pacific Microwave Conference*. 570–572.

[48] Yao Peng, Longfei Shangguan, Yue Hu, Yujie Qian, Xianshang Lin, Xiaojiang Chen, Dingyi Fang, and Kyle Jamieson. 2018. PLoRa: a passive long-range data network from ambient LoRa transmissions. In *Proceedings of the 2018 Conference of the ACM Special Interest Group on Data Communication* (Budapest, Hungary) *(SIGCOMM '18)*. Association for Computing Machinery, New York, NY, USA, 147–160. https://doi.org/10.1145/3230543.3230567

[49] Hossein Pirayesh, Shichen Zhang, Pedram Kheirkhah Sangdeh, and Huacheng Zeng. 2022. MaLoRaGW: Multi-User MIMO Transmission for LoRa. In *Proceedings of the 20th ACM Conference on Embedded Networked Sensor Systems*. 179–192.

[50] Hossein Pirayesh, Shichen Zhang, Pedram Kheirkhah Sangdeh, and Huacheng Zeng. 2023. MaLoRaGW: Multi-User MIMO Transmission for LoRa. In *Proceedings of the 20th ACM Conference on Embedded Networked Sensor Systems* (Boston, Massachusetts) *(SenSys '22)*. Association for Computing Machinery, New York, NY, USA, 179–192. https://doi.org/10.1145/3560905.3568533

[51] Hariharan Shankar Rahul, Swarun Kumar, and Dina Katabi. 2012. JMB: Scaling wireless capacity with user demands. *ACM SIGCOMM Computer Communication Review* 42, 4 (2012), 235–246.

[52] RAKwireless. [n. d.]. RAK7289 V2 Datasheet. https://docs.rakwireless.com/Product-Categories/WisGate/RAK7289-V2/Datasheet/, year = 2024, note = Accessed: 2024-08-14.

[53] Yidong Ren, Wei Sun, Jialuo Du, Huaili Zeng, Younsuk Dong, Mi Zhang, Shigang Chen, Yunhao Liu, Tianxing Li, and Zhichao Cao. 2024. Demeter: Reliable Cross-soil LPWAN with Low-cost Signal Polarization Alignment. In *Proceedings of the 30th Annual International Conference on Mobile Computing and Networking*. 230–245.

[54] Ralph Schmidt. 1986. Multiple emitter location and signal parameter estimation. *IEEE transactions on antennas and propagation* 34, 3 (1986), 276–280.

[55] Semtech. 2020. *SX1276 Datasheet*. Retrieved May, 2020 from https://www.semtech.com/products/wireless-rf/lora-connect/sx1276

[56] Muhammad Osama Shahid, Daniel Koch, Jayaram Raghuram, Bhuvana Krishnaswamy, Krishna Chintalapudi, and Suman Banerjee. 2024. {Cloud-LoRa}: Enabling Cloud Radio Access {LoRa} Networks Using Reinforcement Learning Based {Bandwidth-Adaptive} Compression. In *21st USENIX Symposium on Networked Systems Design and Implementation (NSDI 24)*. 1959–1976.

[57] Muhammad Osama Shahid, Millan Philipose, Krishna Chintalapudi, Suman Banerjee, and Bhuvana Krishnaswamy. 2021. Concurrent interference cancellation: decoding multi-packet collisions in LoRa. In *Proceedings of the 2021 ACM SIGCOMM 2021 Conference* (Virtual Event, USA) *(SIGCOMM '21)*. Association for Computing Machinery, New York, NY, USA, 503–515. https://doi.org/10.1145/3452296.3472931

[58] Wei-Liang Shen, Yu-Chih Tung, Kuang-Che Lee, Kate Ching-Ju Lin, Shyamnath Gollakota, Dina Katabi, and Ming-Syan Chen. 2012. Rate adaptation for 802.11 multiuser MIMO networks. In *Proceedings of the*

18th annual international conference on Mobile computing and networking. 29–40.

[59] Clayton Shepard, Hang Yu, Narendra Anand, Erran Li, Thomas Marzetta, Richard Yang, and Lin Zhong. 2012. Argos: Practical many-antenna base stations. In *Proceedings of the 18th annual international conference on Mobile computing and networking*. 53–64.

[60] Kyungseop Shin, Ieryung Park, Junhee Hong, Dongsoo Har, and Dongho Cho. 2015. Per-node throughput enhancement in Wi-Fi densenets. *IEEE Communications Magazine* 53, 1 (2015), 118–125. https://doi.org/10.1109/MCOM.2015.7010524

[61] Q.H. Spencer, A.L. Swindlehurst, and M. Haardt. 2004. Zero-forcing methods for downlink spatial multiplexing in multiuser MIMO channels. *IEEE Transactions on Signal Processing* 52, 2 (2004), 461–471. https://doi.org/10.1109/TSP.2003.821107

[62] Kun Tan, He Liu, Ji Fang, Wei Wang, Jiansong Zhang, Mi Chen, and Geoffrey M Voelker. 2009. SAM: enabling practical spatial multiple access in wireless LAN. In *Proceedings of the 15th annual international conference on Mobile computing and networking*. 49–60.

[63] Suhua Tang, Akio Hasegawa, Riichiro Nagareda, Akito Kitaura, Tatsuo Shibata, and Sadao Obana. 2011. Improving throughput of wireless LANs with transmit power control and slotted channel access. In *2011 IEEE 22nd International Symposium on Personal, Indoor and Mobile Radio Communications*. 834–838. https://doi.org/10.1109/PIMRC.2011.6140084

[64] Shuai Tong, Jiliang Wang, and Yunhao Liu. 2020. Combating packet collisions using non-stationary signal scaling in LPWANs. In *Proceedings of the 18th International Conference on Mobile Systems, Applications, and Services*. 234–246.

[65] Shuai Tong, Jiliang Wang, Jing Yang, Yunhao Liu, and Jun Zhang. 2024. Citywide LoRa Network Deployment and Operation: Measurements, Analysis, and Implications. In *Proceedings of the 21st ACM Conference on Embedded Networked Sensor Systems* (Istanbul, Turkiye) *(SenSys '23)*. Association for Computing Machinery, New York, NY, USA, 362–375. https://doi.org/10.1145/3625687.3625796

[66] Shuai Tong, Zhenqiang Xu, and Jiliang Wang. 2020. Colora: Enabling multi-packet reception in lora. In *IEEE INFOCOM 2020-IEEE Conference on Computer Communications*. IEEE, 2303–2311.

[67] Y.-P. Eric Wang, Xingqin Lin, Ansuman Adhikary, Asbjorn Grovlen, Yutao Sui, Yufei Blankenship, Johan Bergman, and Hazhir S. Razaghi. 2017. A Primer on 3GPP Narrowband Internet of Things. *IEEE Communications Magazine* 55, 3 (2017), 117–123. https://doi.org/10.1109/MCOM.2017.1600510CM

[68] K. Whitehouse, A. Woo, F. Jiang, J. Polastre, and D. Culler. 2005. Exploiting the capture effect for collision detection and recovery. In *The Second IEEE Workshop on Embedded Networked Sensors, 2005. EmNetS-II.* 45–52. https://doi.org/10.1109/EMNETS.2005.1469098

[69] Kamin Whitehouse, Alec Woo, Fred Jiang, Joseph Polastre, and David Culler. 2005. Exploiting the capture effect for collision detection and recovery. In *The Second IEEE Workshop on Embedded Networked Sensors, 2005. EmNetS-II.* IEEE, 45–52.

[70] Starsky H. Y. Wong, Hao Yang, Songwu Lu, and Vaduvur Bharghavan. 2006. Robust rate adaptation for 802.11 wireless networks. In *Proceedings of the 12th Annual International Conference on Mobile Computing and Networking* (Los Angeles, CA, USA) *(MobiCom '06)*. Association for Computing Machinery, New York, NY, USA, 146–157. https://doi.org/10.1145/1161089.1161107

[71] Haifeng Wu and Yu Zeng. 2014. Passive RFID tag anticollision algorithm for capture effect. *IEEE sensors journal* 15, 1 (2014), 218–226.

[72] Xianjin Xia, Qianwu Chen, Ningning Hou, and Yuanqing Zheng. 2023. HyLink: Towards High Throughput LPWANs with LoRa Compatible Communication. In *Proceedings of the 20th ACM Conference on Embedded Networked Sensor Systems* (Boston, Massachusetts) *(SenSys '22)*. Association for Computing Machinery, New York, NY, USA, 578–591. https://doi.org/10.1145/3560905.3568516

[73] Xianjin Xia, Qianwu Chen, Ningning Hou, Yuanqing Zheng, and Mo Li. 2023. XCopy: Boosting Weak Links for Reliable LoRa Communication. In *Proceedings of the 29th Annual International Conference on Mobile Computing and Networking* (Madrid, Spain) *(ACM MobiCom '23)*. Association for Computing Machinery, New York, NY, USA, Article 14, 15 pages. https://doi.org/10.1145/3570361.3592516

[74] Xianjin Xia, Ningning Hou, Yuanqing Zheng, and Tao Gu. 2021. PCube: Scaling LoRa Concurrent Transmissions with Reception Diversities. In *Proceedings of the 27th Annual International Conference on Mobile Computing and Networking (MobiCom'21)*. ACM.

[75] Xianjin Xia, Yuanqing Zheng, and Tao Gu. 2019. FTrack: parallel decoding for LoRa transmissions. In *Proceedings of the 17th Conference on Embedded Networked Sensor Systems* (New York, New York) *(SenSys '19)*. Association for Computing Machinery, New York, NY, USA, 192–204. https://doi.org/10.1145/3356250.3360024

[76] Xianjin Xia, Yuanqing Zheng, and Tao Gu. 2021. LiteNap: Downclocking LoRa Reception. *IEEE/ACM Transactions on Networking* 29, 6 (2021), 2632–2645. https://doi.org/10.1109/TNET.2021.3096990

[77] Binbin Xie, Minhao Cui, Deepak Ganesan, Xiangru Chen, and Jie Xiong. 2023. Boosting the long range sensing potential of lora. In *Proceedings of the 21st Annual International Conference on Mobile Systems, Applications and Services*. 177–190.

[78] Binbin Xie, Deepak Ganesan, and Jie Xiong. 2022. Embracing lora sensing with device mobility. In *Proceedings of the 20th ACM Conference on Embedded Networked Sensor Systems*. 349–361.

[79] Xiufeng Xie and Xinyu Zhang. 2014. Scalable user selection for MU-MIMO networks. In *IEEE INFOCOM 2014-IEEE Conference on Computer Communications*. IEEE, 808–816.

[80] Zhenqiang Xu, Shuai Tong, Pengjin Xie, and Jiliang Wang. 2023. From Demodulation to Decoding: Toward Complete LoRa PHY Understanding and Implementation. *ACM Trans. Sen. Netw.* 18, 4, Article 64 (Jan. 2023), 27 pages. https://doi.org/10.1145/3546869

[81] Taesang Yoo, Nihar Jindal, and Andrea Goldsmith. 2007. Multi-antenna downlink channels with limited feedback and user selection. *IEEE Journal on Selected Areas in Communications* 25, 7 (2007), 1478–1491.

[82] Shiming Yu, Xianjin Xia, Ningning Hou, Yuanqing Zheng, and Tao Gu. 2024. Revolutionizing LoRa Gateway with XGate: Scalable Concurrent Transmission across Massive Logical Channels. In *Proceedings of the 30th Annual International Conference on Mobile Computing and Networking* (Washington D.C., DC, USA) *(ACM MobiCom '24)*. Association for Computing Machinery, New York, NY, USA, 482–496. https://doi.org/10.1145/3636534.3649375

[83] Shiming Yu, Xianjin Xia, Ziyue Zhang, Ningning Hou, and Yuanqing Zheng. 2024. FDLoRa: Tackling Downlink-Uplink Asymmetry with Full-duplex LoRa Gateways. In *Proceedings of the 22nd ACM Conference on Embedded Networked Sensor Systems* (Hangzhou, China) *(SenSys '24)*. Association for Computing Machinery, New York, NY, USA, 281–294. https://doi.org/10.1145/3666025.3699338

[84] Talha Zahir, Kamran Arshad, Atsushi Nakata, and Klaus Moessner. 2013. Interference Management in Femtocells. *IEEE Communications Surveys & Tutorials* 15, 1 (2013), 293–311. https://doi.org/10.1109/SURV.2012.020212.00101

[85] Renjie Zhao, Timothy Woodford, Teng Wei, Kun Qian, and Xinyu Zhang. 2020. M-cube: A millimeter-wave massive MIMO software radio. In *Proceedings of the 26th Annual International Conference on Mobile Computing and Networking*. 1–14.